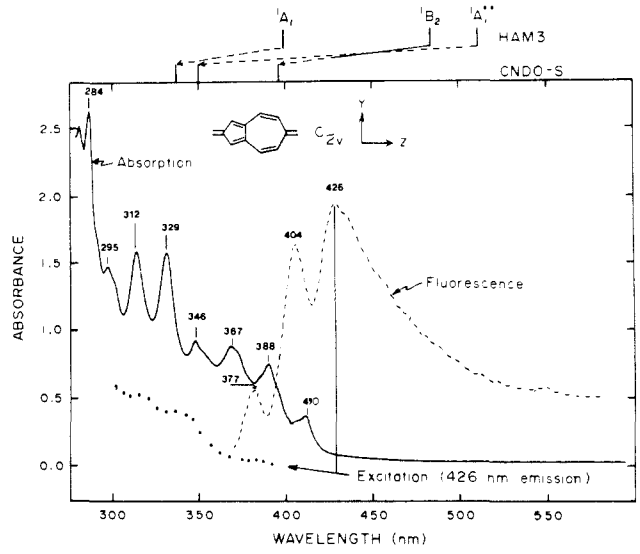

Figure 2. Absorption, fluorescence, and excitation (426-nm emission) of 3-methylpentane solutions of **1** at low (<−80 °C) temperature. HAM3/CI and CNDO/S estimates of the vertical excitation energies are shown by bars at the top ($^1A_1$** designates excitation state with a large contribution from electron pair (two electron) promotion).

as from the Hofmann elimination (Scheme I), supporting the notion that **1** is indeed an intermediate in the formation of **5** under those conditions.

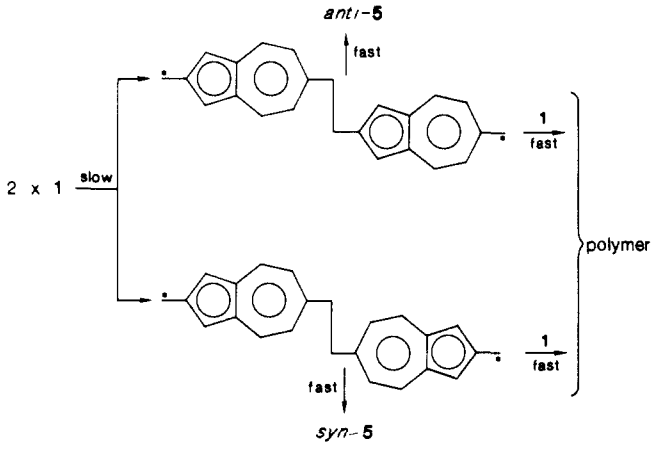

The fluorescence spectrum shown in Figure 2 was obtained after subtraction of contributions from fluorescent impurities and the products of reaction of **1**. The emitting species, responsible for this part of Figure 2, was found to disappear with an apparent second-order rate constant that was approximately the same as the value (relative) found for the absorbing species (**1**). This observation suggests that the fluorescence depicted in Figure 2 is also due to **1**. If that is the case then it suggests at least two excited states in the 300–420-nm absorption region with emission from the higher one. 2,6-Azulylene (**1**) would then be another example of a system exhibiting (anti-Kasha)[9] fluorescence from a higher than first excited state (at least in part). The preliminary[10] excitation spectrum (Figure 2) supports this rationalization.

The Raman (457.9-nm excitation) spectrum of THF solution (−40 °C) of the FVP condensate of **5** shows five clear maxima in the C–C valence stretching region (1600, 1514, 1480, 1463, and 1446 cm^{-1}) after corrections for solvent and reaction product background. This spectrum also supports the assignment of the FVP products structure as **1**. Five resonance enhanced fundamentals are expected if the lowest (410-nm onset, Figure 2) transition is $^1B_2$. However, additional spectra at varying excitation frequencies would be required before such an assignment could be considered secure.

Figure 2 shows the predictions of the vertical excitation energies of the first several singlet excited states of **1** using CNDO/S[11] and HAM3/CI[12] models. Both models agree that at least two (essentially) single electron excitation states ($^1A_1$, $^1B_2$), and one state containing a significant population of a two-electron excitation ($^1A_1$**) should be located in the 300–510-nm region of the spectrum. The CNDO/S calculations[11a] are in reasonably good accord with the superficial absorption band shape. The HAM/3 procedure appears to underestimate the HOMO–LUMO gap to a considerable extent.

In summary, we believe we have provided an efficient way to obtain **1**. The stability of this reactive polyene is sufficient to allow good spectroscopic characterization. The CNDO/S calculations suggest that the ordering of the first two of its one-electron-promoted states is $^1B_2$ lower than $^1A_1$.[13] We hope to be able to examine the spectral properties of **1** in greater detail, especially its photoelectron spectrum which may reveal, in an unambiguous manner, the many electron effects predicted by the non-Koopmans[14] model.

Acknowledgment. We are grateful to the National Science Foundation for grants supporting this research.

(9) Sugihara, Y.; Wakabayashi, S.; Murata, I.; Jingiyi, M.; Nakazawa, T.; Persy, G.; Wirz, J. *J. Am. Chem. Soc.* **1985**, *1047*, 5894. Geldof, P. A.; Rettschnick, R. P. H.; Hoytink, G. J. *Chem. Phys. Lett.* **1967**, *4*, 59. Easterly, C. E.; Christophorou, L. G.; Blaunstein, R. P.; Carter, J. G. *Ibid* **1970**, *6*, 579.

(10) The high reactivity of **1** complicates the interpretation of the excitation spectra. The most significant observation is the disappearance of excitation of the strong 404- and 425-nm emission lines at excitation wavelengths greater than 380 nm.

(11) Ellis, R. L.; Kuehnlenz, G.; Jaffe, H. H. *Theor. Chim. Acta* **1972**, *26*, 131. Quantum Chemistry Program Exchange, Indiana University, Bloomington, IN 47401, QCPE No. 174. (a) The double electron promoted configurations in CNDO/s were approximated through a small CI calculation including the lowest 10 excited configurations and the neutral ground state.

(12) Lindholm, E. *Lecture Notes in Chemistry*; Springer Verlag: Berlin, 1985. Asbrink, L.; Fridh, C.; Lindholm, E.; DeBruijn, S. *Chem. Phys. Lett.* **1979**, *66*, 411.

(13) This ordering is dominated by the two electron integrals. The $^1A_1$ transition corresponds to the HOMO–LUMO promotion in CNDO/S.

(14) Koenig, T.; Klopfenstein, C. E.; Southworth, S.; Hoobler, J. A.; Wielesek, R. A.; Balle, T.; Snell, W.; Imre, D. *J. Am. Chem. Soc.* **1983**, *105*, 2256.

Hydrophobic Perturbation of Acyclic Equilibria

Ned A. Porter,* Dong Ok, Christopher M. Adams, and Jeffrey B. Huff

Department of Chemistry, Duke University
Durham, North Carolina 27706

Received April 14, 1986

Many enzymatic processes occur at interfaces between aqueous and hydrophibic media. Stereoselectivity in many of these conversions has been attributed to hydrophobic forces that favor the formation of one stereoisomeric form.[1,2] While there has been a considerable effort expended to understand the nature of the hydrophobic effect in biological systems such as lipid bilayer membranes, studies directed at revealing the influence of amphiphilic aggregates such as micelles and bilayers on organic stereochemistry are relatively rare.[3-5] We have recently reported that molecular aggregates dramatically influence the stereo-

(1) Israelachvili, J. N. *Intermolecular and Surface Forces*; Academic Press: New York, 1985.

(2) Fendler, J. H. *Membrane Mimetic Chemistry*; Wiley: New York, 1982.

(3) Stewart, M. V.; Arnett, E. M. *Top. Stereochem.* **1982**, *13*, 195.

(4) Ueoka, R.; Moss, R. A.; Swarup, S.; Matsumoto, Y.; Straus, G.; Murakami, Y. *J. Am. Chem. Soc.* **1985**, *107*, 2185–2186.

(5) Nakashima, N.; Asakuma, S.; Kunitake, T. *J. Am. Chem. Soc.* **1985**, *107*, 509–510.

0002-7863/86/1508-5025$01.50/0

chemical course of reactions involving intermediate radical pairs,[6] and we concluded that molecular aggregation can control the stereochemical course of kinetic processes such as radical pair coupling. It is reasonable to expect that aggregation effects might perturb organic stereoisomeric equilibria as well, but few studies have been directed toward systematically investigating this possibility. We report here the results of such a study.

We have chosen the dicarboxylic acids **1** (meso and *dl*), **2** (meso and *dl*), and the dienone **3** (meso and *dl*) for study since we

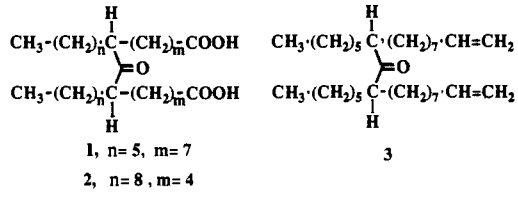

anticipate that **1** and **2** will form molecular aggregates in aqueous media while **3** serves as a touchstone for reactions carried out in isotropic media without the possibility of aggregates being formed. Each of these compounds has an epimerizable stereocenter which provides a means for investigating equilibrium between the stereoisomers. The meso and *dl* isomers of **1** and **2** could be readily separated by reverse-phase high-pressure liquid chromatography on C-18 columns with solvent acetonitrile/water/acetic acid, 95/5/.1, the meso stereoisomer eluting last for both **1** and **2**.[7] The diacids were prepared by straightforward methods (vide infra) and all intermediates in the synthesis were fully characterized by spectroscopy and elemental analysis.[8,9]

The meso and *dl* stereoisomers of the dienone **3** could be separated by gas chromatography on a 30-m SP-2330 fused silica capillary column,[10] but they could not be separated on a preparative scale by any of the normal chromatographic procedures. Quantities of the separated stereoisomeric *meso*- and *dl*-**3** could be obtained by chromatography of the corresponding dialdehydes on silica gel (hexane/EtOAc, 96/4) followed by conversion of the purified dialdehydes to the isomeric dienones **3**, with methylene Wittig reagent. Single-crystal X-ray analysis of the diacids *meso*-**1** and *meso*-**2** identified these stereoisomers and this assignment of stereochemistry was used by correlation to identify the stereoisomers of **3**.[11]

The stereoisomers of diacids **1** and **2** all form soapy solutions in aqueous base at concentrations above 10^{-4} M.[12] At 60 °C, epimerization of the diastereomers occurs over the course of several days, equilibrium being reached for 1 mM *meso*- or *dl*-**1** in 1 M KOH after 200 h. Analysis of the equilibrium product mixture was readily obtained by acidifying to pH 4, extracting with dichloromethane or ether, and performing analytical reverse-phase chromatography on a C-18 column. Equilibration of the diacids was also achieved in 1 M KOH containing the ammonium surfactants cetyltrimethylammonium bromide (CTAB) or dicetyldimethylammonium bromide (DDAB). In these experiments, the ammonium surfactant diacid ratio was 20/1 and the experiments were carried out at concentrations significantly above the cmc of the ammonium surfactant. Analysis of the equilibration mixture in ammonium surfactants required conversion of the diacids to the dimethyl esters with diazomethane before extraction and HPLC analysis.[13] We have not yet measured the rates of the equilibrations but we note that the ammonium surfactants catalyze the approach to equilibrium, CTAB promoting the equilibration in less than 24 h. Equilibrium values for epimerizations of **1**–**3** are presented in Table I. Equilibrations were also carried out with other bases such as sodium, rubidium, and cesium hydroxide and for concentrations of the diacid **2** from 10^{-2} to 10^{-4} M. A change of base or concentration did not lead to significant changes in the equilibrium ratios obtained.

Table I. Equilibration in Water, Micelles, and Bilayers (T 60 °C)

starting diastereomer[a] (concn), mM	surfactant 1 M KOH (R_4NBr/diacid)	meso/*dl*
dl-**1** (1)	none	72/28±1
meso-**1** (1)	none	72/28±1
dl-**1** (5)	CTAB[b] (20/1)	66/34±1
meso-[1] (5)	CTAB[b] (20/1)	65/35±1
dl-**1** (5)	DDAB[c] (20/1)	82/18±1
meso-**1** (5)	DDAB[c] (20/1)	81/19±1
dl-**2** (1)	none	82/18±1
meso-**2** (1)	none	82/18±1
dl-**2** (5)	CTAB[b] (20/1)	84/16±1
meso-**2** (5)	CTAB[b] (20/1)	84/16±2
dl-**2** (5)	DDAB[c] (20/1)	89/11±1
meso-**2** (5)	DDAB[c] (20/1)	89/11±2
dl-**3** (25)	benzene/DBU	48/52±1
meso-**3** (25)	benzene/DBU	49/51±1

[a] Triplicate analysis of at least duplicate experiments for each diastereomer. [b] Cetyltrimethylammonium bromide. [c] Dicetyldimethylammonium bromide.

The data presented in Table I suggest that the equilibrium stereoisomer ratio can be significantly altered by the medium of the equilibration. The dienone **3** equilibrates to a 1/1 meso/*dl* product ratio in benzene indicating that there is no stereochemical bias for one orientation of the C_6H_{13} and the C_9H_{17} substituents at the stereocenters. Classical stereochemical effects thus lead to no diastereoselection for **3**. The equilibrations of **1** and **2** in water, on the other hand, indicate that significant diastereoselection may be imposed on the system by the aqueous medium and by ammonium surfactants. We are aware of no previous reports that anticipate these results or suggest that the meso stereoisomer would be preferred at equilibrium in water. The extent of the diastereoselectivity depends on the substrate and the nature of the aggregates formed from each substrate. The contrast between the diacids **1** and **2** is particularly striking in their response to added ammonium salts as cosurfactants. While **1** equilibrates to a 72/28 meso/*dl* equilibrium in 1 M KOH alone, the selectivity is reduced to 65/35 by mixing with CTAB, a surfactant known to form micellar aggregates.[14] On the other hand, equilibration in mixtues of **1** and DDAB results in an enhanced diastereoselectivity of 82/18. For the diacid **2**, diastereoselectivities in water alone and with added CTAB cosurfactant are comparable (82/18) while DDAB again enhances diastereoselectivity to 89/11. The ordered liquid-crystalline environment of DDAB bilayers[15] apparently enforces formation of the meso stereoisomer.

The results of this study point to the potential importance of the hydrophobic effect in controlling acyclic stereochemistry. In contrast to analogous systems, i.e., **3**, where classical stereo-

(6) Porter, N. A.; Arnett, E. M.; Brittain, W. J.; Johnson, E. A.; Krebs, P. J. *J. Am. Chem. Soc.* **1986**, *108*, 1014–1018.

(7) Preparative HPLC was carried out on a Rainin Dynamax C-18 column with 95/5/0.1 acetonitrile/water/acetic acid and a flow rate of 9 mL/min. The *dl* diastereomer eluted first for both **1** and **2**.

(8) ^1H and ^{13}C NMR spectra, mass spectra, and C and H analysis support the structures of **1**–**3** and all intermediates (except aldehydes which proved to be too unstable to give acceptable C and H analysis).

(9) Dienone **3** was oxidatively cleaved to give the corresponding dialdehyde which was oxidized to the dicarboxylic acid **1** with Jones reagent. The dienone **3** was prepared by coupling the dianion of 2-pentyl-10-undecenoic acid (LDA) with the acid chloride of the same acid followed by decarboxylation of the product β-keto acid (180°).

(10) Supelco, Inc.: 30 m × 0.25 mm i.d. Column temp = 185 °C; retention times meso = 65 min, *dl* = 68 min.

(11) Single-crystal X-ray analyses were performed by Dr. A. T. McPhail of the Duke University Structure Center and will be subsequently published.

(12) Light-scattering and surface-tension experiments carried out in this laboratory (K. Kim and G. Brelsford) indicate aggregation of **1** occurs at concentrations above 10^{-6} M. The results of this study will be published in due course.

(13) The workup procedure for CTAB and DDAB experiments is as follows: After acidification with 10% HCl, water was removed from the CTAB or DDAB solution by evaporation with benzene used to azeotrope the last traces of water. Diazomethane in ether was added to the residue and the resulting solution was chromatographed on silica with EtOAc. Control experiments verify that accurate analyses may be obtained by this procedure.

(14) See, for example: Cipriciani, A.; Germani, R.; Savelli, G.; Bunton, C. A. *J. Chem. Soc., Perkin Trans 2* **1982**, 527–529.

(15) (a) Shimomura, M.; Kunitake, T. *Chem. Lett.* **1981**, 1001–1004. (b) Okahata, Y.; Ando, R.; Kunitake, T. *Ber. Bunsenges. Phys. Chem.* **1981**, *85*, 789–798.

chemical effects lead to a 1/1 product mixture, the carboxylate substituents on **1** and **2** remote from the stereocenters by several methylene units impose a diastereomer selection of up to 8/1. The success of this first attempt to study acyclic equilibrium stereoenforcement encourages a more thorough investigation of the phenomenon.

Acknowledgment. N.A.P. gratefully acknowledges grants from NIH (HL 17921), NSF, and Burroughs Wellcome to support this research. Helpful discussions with Ron Grunwald and Dr. George Painter are also much appreciated.

(16) **Note Added in Proof**: The diacid **1** equilibrates to a 50/50 mixture of diastereomers in benzene at 60 °C in a reaction catalyzed by toluenesulfonic acid.

A Binuclear Iron Peroxide Complex Capable of Olefin Epoxidation

Bruce P. Murch, Fontaine C. Bradley, and Lawrence Que, Jr.*

Department of Chemistry, University of Minnesota Minneapolis, Minnesota 55455

Received March 31, 1986

Nature has utilized structurally similar metalloprotein sites for reversible oxygen binding and for oxygen activation; myoglobin and cytochrome P450 constitute one such carrier/activator pair which has heme sites,[1] while hemocyanin and tyrosinase have binuclear copper sites.[2] There are as yet no examples of a binuclear nonheme iron dioxygen activating enzyme corresponding to hemerythrin,[3] though methane monooxygenase may have such a site on the basis of the similarity of its EPR spectrum with those of semimethemerythrins.[4] Based on this analogy, we are studying the capability of synthetic binuclear iron complexes to activate the O-O bond, and we report our initial results in this paper.

The complex $(Me_4N)[Fe_2L(OAc)_2]$[5] is obtained by addition of acetate at pH 5 to $[Fe_2L(OH)(H_2O)_2]$[6] and metathesis with Me_4NCl. X-ray crystallography[7] shows that the phenolate and the two acetates bridge the iron centers to give a confacial bioctahedral structure (Figure 1) similar to that found for $[(HBpz_3Fe)_2OH(OAc)_2]^+$.[8] This triply bridging unit appears to be a common structural feature for binuclear complexes[9] and

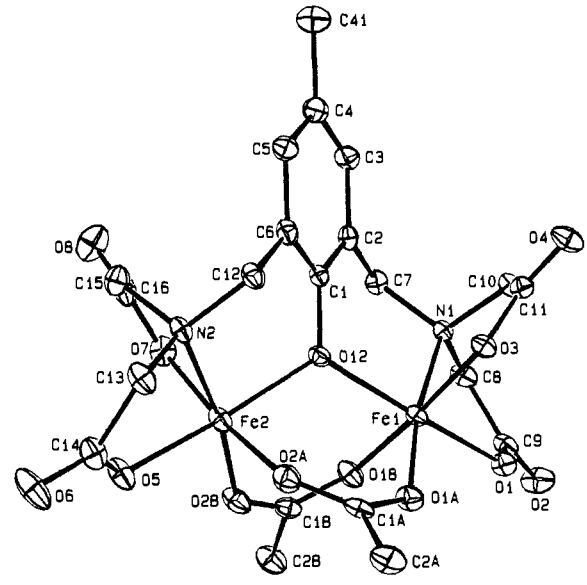

Figure 1. ORTEP plot of the structure of $[Fe_2L(OAc)_2]^-$, showing 50% probability ellipsoids. Representative distances (Å): Fe1-O12, 1.997 (2); Fe2-O12, 2.019 (2); Fe1-N1, 2.151 (2); Fe2-N2, 2.158 (2); Fe1-O1, 1.996 (2); Fe1-O3, 1.966 (2); Fe2-O5, 1.973 (2); Fe2-O7, 1.954 (2); Fe1-O1A, 1.970 (2); Fe1-O1B, 2.050 (2); Fe2-O2A; 2.049 (2); Fe2-O2B, 1.970 (2); Fe1-Fe2, 3.442 (0). Angle Fe1-O12-Fe2, 117.9 (1)°.

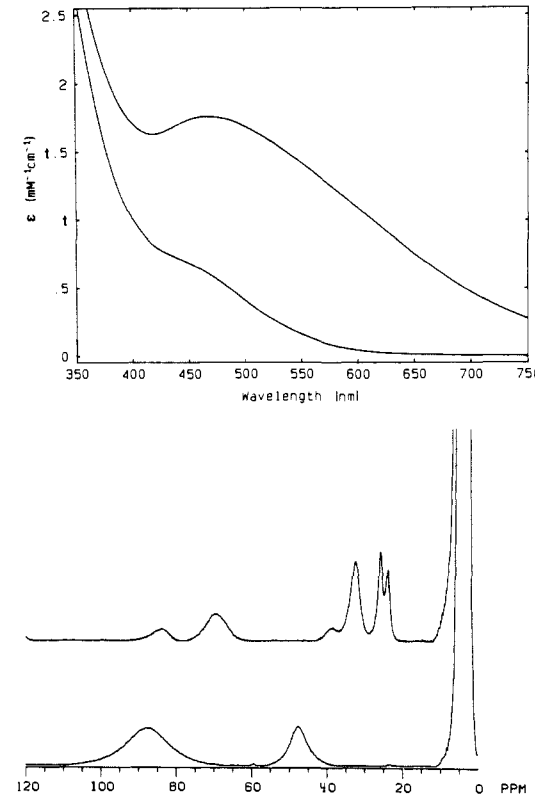

Figure 2. (Top) Visible spectra of 0.72 mM $[Fe_2L'(OAc)_2]^-$ (lower trace) and 0.72 mM $[Fe_2L'(OAc)_2]^-$ + 0.2 M H_2O_2 (upper trace) in methanol with 50 mM 1:1 HOAc/NaOAc. (Bottom) ^1H NMR spectra of $[Fe_2L'(OAc)_2]^-$ in MeOH-d_4 with 50 mM HOAc/NaOAc (lower trace) and $[Fe_2L'(OAc)_2]^-$ + H_2O_2 in Me_2SO-d_6 with 50 mM HOAc/NaOAc (upper trace).

(1) Groves, J. T. *Adv. Inorg. Biochem.* **1979**, *1*, 119-145. White, R. E.; Coon, M. J. *Annu. Rev. Biochem.* **1980**, *49*, 315-356.

(2) Himmelwright, R. S.; Eickman, N. C.; LuBien, C. D.; Lerch, K.; Solomon, E. I. *J. Am. Chem. Soc.* **1980**, *102*, 7339-7344. Eickman, N. C.; Solomon, E. I.; Larrabee, J. A.; Spiro, T. G.; Lerch, K. *J. Am. Chem. Soc.* **1978**, *100*, 6529-6531.

(3) Stenkamp, R. E.; Sieker, L. C.; Jensen, L. H.; McCallum, J. D.; Sanders-Loehr, J. *Proc. Natl. Acad. Sci. U.S.A.* **1985**, *82*, 713-716.

(4) Woodland, M. P.; Dalton, H. *J. Biol. Chem.* **1984**, *259*, 53-59. Woodland, M. P.; Cammack, R. In *Microbial Gas Metabolism: Mechanistic, Metabolic and Biotechnological Aspects*; Poole, R. K., Dow, C. S., Eds.; Academic Press: New York, 1985; pp 209-213.

(5) Abbreviations: L, *N,N'*-(2-hydroxy-5-methyl-1,3-xylylene)bis(*N*-carboxymethylglycine); OAc, acetate; $HBpz_3$, hydrotris(pyrazolyl)borate; L', *N,N'*-(2-hydroxy-5-chloro-1,3-xylylene)bis(*N*-carboxymethylglycine); bpmp, 2,6-bis[[bis(2-pyridylmethyl)amino]methyl]-4-methylphenol; acac, acetylacetonate; TPP, *meso*-tetraphenylporphin; OTf, triflate; EDTA, *N,N,N',N'*-ethylenediaminetetraacetate; Cl_2HDA, *N*-(4,6-dichloro-2-hydroxybenzyl)-*N*-(carboxymethyl)glycine.

(6) Murch, B. P.; Boyle, P. D.; Que, L., Jr. *J. Am. Chem. Soc.* **1985**, *107*, 6728-6729.

(7) The complex crystallized out of water as $(Me_4N)[Fe_2L(OAc)_2]\cdot H_2O$ in the monoclinic space group $P2_1/a$ with the following cell constants: *a*, 25.963 (15) Å; *b*, 9.603 (3) Å; *c*, 12.278 (3) Å; β, 96.34 (3)°. The structure was determined from 2304 out of a total of 4878 reflections with r = 3.56% and r_w = 3.99%. Complete details of the structure will be published elsewhere. Elemental analysis for $(Me_4N)[Fe_2L(OAc)_2]\cdot H_2O$ calculated for $C_{25}H_{37}Fe_2N_3O_{14}$: C, 41.98; H, 5.21; N, 5.91. Found: C, 41.86; H, 5.23; N, 5.87.

(8) Armstrong, W. H.; Lippard, S. J. *J. Am. Chem. Soc.* **1984**, *106*, 4632-4633.

0002-7863/86/1508-5027$01.50/0